ISSN 1330-3651 (Print), ISSN 1848-6339 (Online)
https://doi.org/10.17559/TV-20210712053027
Original scientific paper

Simulation and Test of Lateral Ballast Resistance to 1435 mm/1000 mm Dual-Gauge Sleepers

Shougang HUANG, Jinjie CHEN, Jianxi WANG*, Bin YAO, Yadong LI

Abstract: The stability of a 1000 mm/1435 mm dual-gauge track is lower than that of a single-gauge track. One of the important factors that affects the stability of the track is the lateral resistance of the track bed. We have established a discrete element simulation model of the dual-gauge sleeper-track bed in PFC to analyse the characteristics of the lateral resistance of the 1000 mm/1435 mm dual-gauge sleeper. With China Type IIIc sleepers as the control group, we carried out the lateral resistance test for the full-scale sleeper model under the same conditions. The research results indicate that the most effective way to increase the lateral resistance of the dual-gauge track bed is to increase the end surface area and bottom area of the sleeper. The application of adjacent sleepers is an effective way to increase the lateral resistance of the track bed further. The research results gained from this study can be used to guide the design of dual-gauge sleepers.

Keywords: discrete element method; dual-gauge railway; lateral ballast resistance; sleeper

1 INTRODUCTION

Different gauges are used for railways in different parts of the world. A country may adopt two gauges - 1000 mm and 1435 mm. Neighbouring countries may also choose to adopt these two gauges. A dual-gauge railway (also known as a Gauntlet-track railway) is a new track structure that allows the passage of trains with two different track gauges that are interlaced as one. The 1000mm/1435mm dual-gauge railway (see Fig. 1a) can be used to connect railways with these two gauges.

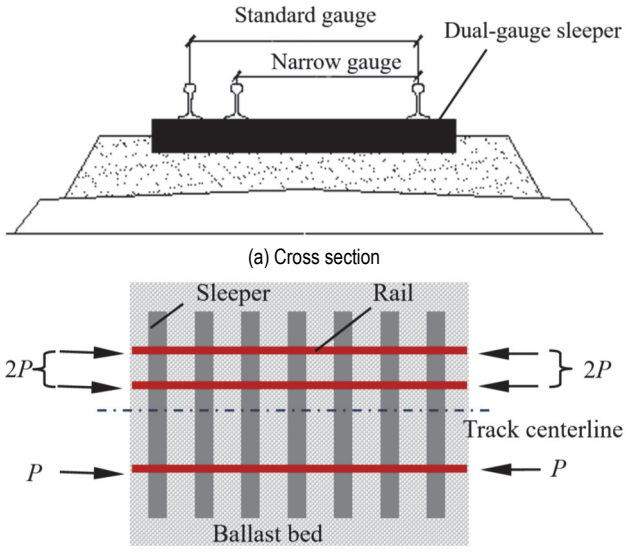

Figure 1 Signal of dual-gauge track

Fig. 2 is a schematic diagram of a 1000 mm/1435mm dual-gauge railway track. It can be seen from the figure that there are two rails on one side of the track centerline and one rail on the other side, which is a very obvious asymmetric feature. When the temperature rises, one steel rail is restricted in the longitudinal direction to produce a temperature stress. This temperature stress is represented as P, and the temperature stress of two steel rails is $2P$. If the track is regarded as a slender rod, the temperature stress will act eccentrically on the track. Compared with a single-gauge railway, a dual-gauge railway has fully locked tracks whose temperature stress increases by about 50% at the same rate of temperature increase. However, its lateral ballast resistance does not increase substantially, making the dual-gauge railway more liable to experience a loss of stability. As the three rails are left-right asymmetric, the track is susceptible to becoming unstable. In order to accommodate for a higher transport capacity, a continuously welded rail track (CWR) should be applied to a dual-gauge railway. In the case of a CWR, sleepers are required to provide large lateral ballast resistance.

How the lateral ballast resistance to sleepers can be increased is an important research aspect in the field of railway engineering. Sadeghi, J. M. et al. [1] studied the influence of mechanical properties of ballast on track maintenance. The research of Esmaeili et al. [2] showed that the steel slag from the iron and steel industry was rougher on the surface and heavier than the ballast currently being used.

Optimising sleeper structure is another way to increase the lateral ballast resistance. Many scholars have studied the characteristics of lateral ballast resistance to different sleepers, including trapezoidal sleepers [3], bi-block sleepers [4], frictional sleepers [5], composite sleepers, steel sleepers, and a variety of other optimised sleepers. Jing Guoqing [6] optimised the shape of China's standard IIIc sleepers. It was found that the lateral ballast resistance to sleepers could be effectively increased by adding side blocks to specific sleeper parts.

With the wide application of the discrete element method, many scholars in China began to use a discrete element numerical simulation software called PFC3D (Particle Flow Code) to study the lateral ballast resistance. Gao Liang et al. [7] used spheres to simulate ballast in PFC3D to examine the influence of bed section size on lateral ballast resistance. Wei Kai et al. [8] studied the lateral resistance to concrete sleepers of a metre-gauge railway using the discrete element method. Jing Guoqing et al. [9] found that when the train speed increased from 200~250 km/h to 300 km/h, the test value and simulation value of lateral ballast resistance dropped by 12.6% and 24.2%, respectively. By using the discrete element method, Xu Yang et al. [10] found that a small size would impair the shear behaviour of the bed.

The dual-gauge sleeper is newly developed, so there is currently a gap in the study of the characteristics of its lateral ballast resistance. In this paper, both tests and simulations are used to study the characteristics of lateral ballast resistance to dual-gauge sleepers.

2 RESISTANCE TEST SCHEME

The dual-gauge sleepers being tested are a structure using reinforced concrete, with a single sleeper weighing 291 kg. The structural dimensions are shown in Fig. 2. A physical dual-gauge railway track is shown in Fig. 3.

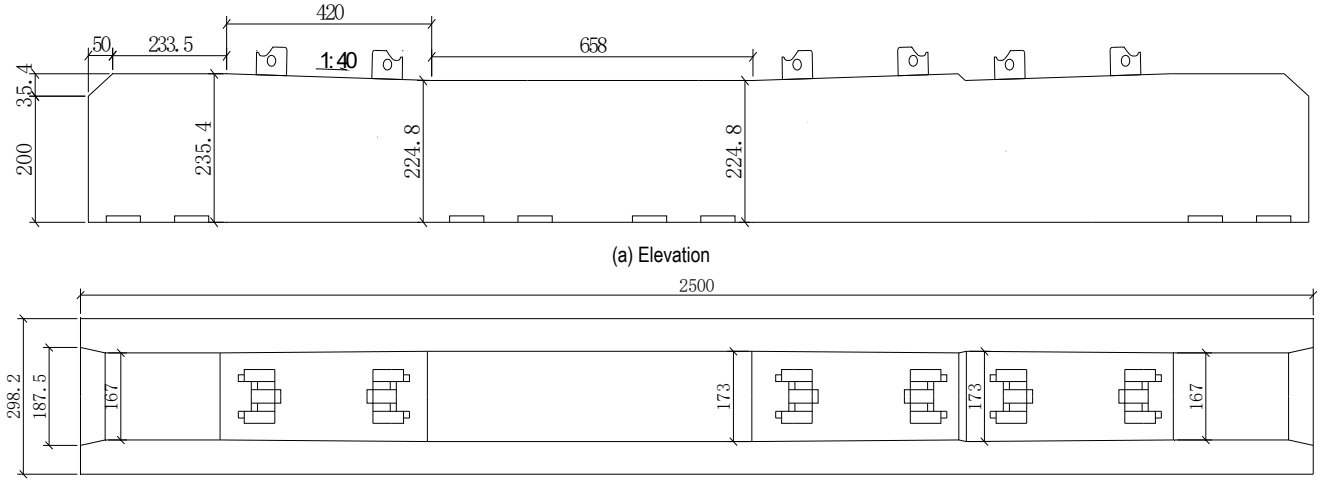

Figure 2 Dimensions of the dual-gauge sleeper / mm

Figure 3 Physical dual-gauge railway

A single control variable is used to control the bed's shoulder width at 500 mm and the bed's slope gradient at 1:1.75; shoulder height is set at 0 mm, 40 mm, 80 mm, 120 mm, 150 mm and 180 mm. The lateral ballast resistance to a dual-gauge sleeper and a IIIc sleeper in China is tested and compared (see Fig. 4). Before each test, sleepers are placed in their original positions, and the bed is tamped six times [11]. Tamping is done the same number of times for each working condition, and the tamping time is also the same. The test is carried out three times under each working condition and the mean value of all three sets of test data is taken.

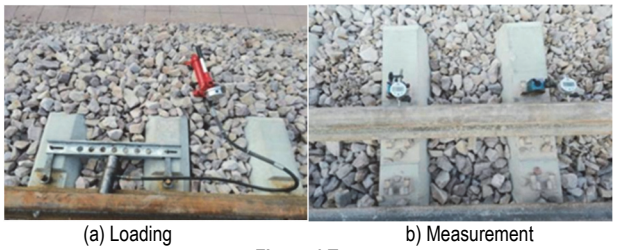

(a) Loading b) Measurement

Figure 4 Test

During the test, the sleeper moves laterally as the jack is pressurised. The dial indicator is used to measure the displacement of the sleeper relative to another rail. The jack pressure is used to load in stages, and the load resistance difference is 1 MPa. After pressure is applied at each step and the reading of the dial indicator remains unchanged [12], the sleeper displacement and the readings are recorded.

3 SIMULATION MODEL BUILDING

3.1 Ballast Simulation Model Building

The spherical shell region with an inner diameter of R_1 and an outer diameter of R_2 is taken as the point cloud generation region, and random variables R_{rand}, α and β are defined. R_{rand}, the distance between a random point and the centre of the sphere, is a random number within (R_1, R_2). α, an angle formed by the line between a random point and the centre of the sphere and the Z axis of the space rectangular coordinate system, is a random number within (0, π). β, an angle formed by the line between a random point and the centre of the sphere and the X axis of the space rectangular coordinate system, is a random number within (0, 2π). The coordinates of the centre of the sphere are (x_0, y_0, z_0). The three-dimensional coordinates of the random point are (x_p, y_p, z_p).

$$\begin{cases} x_p = x_0 + R_{rand} \times \sin\alpha\cos\beta \\ y_p = y_0 + R_{rand} \times \sin\alpha\cos\beta \\ z_p = z_0 + R_{rand} \times \cos\beta \end{cases} \quad (1)$$

Massive random points form a point cloud which generates convex hulls after convex hull computing. The convex hulls generated are filled with spheres featuring different radii to produce particle clumps, thereby simulating the ballast (as shown in Fig. 5).

Figure 5 Simulation model of ballast

Then, the simulated ballast is randomly shaped, and a bed simulation model is built.

3.2 Sleeper Simulation Model Building

Koike Y. et al. 0 used particle clump elements and Xiao J. et al. 0 applied wall elements to simulate sleepers, both gaining simulation results consistent with the test results. However, in this paper, for the building of a sleeper simulation model based on the discrete element method, the shape of sleepers is directly generated in the software PFC according to contour feature points (see Fig. 6).

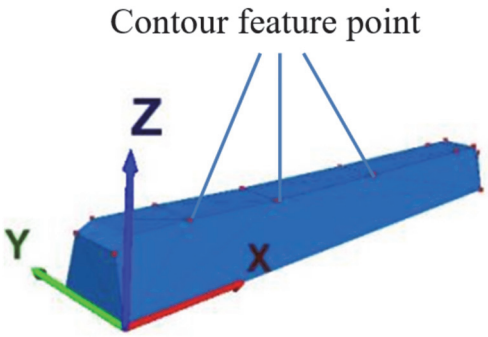

Figure 6 Sleeper simulation

The intersection of the right edge line and the near-end edge line at the bottom of the sleeper is taken as the coordinates origin, and the *X*, *Y* and *Z* axes are set along the length, width and height directions of the sleeper, respectively. Suppose the sleeper has a length of l and a width of w and assume that the coordinates of a certain point are (x_p, y_p, z_p). Then the coordinates of the left and right symmetric points are $(l-x_p, y_p, z_p)$, and the coordinates of the front and rear symmetric points are $(x_p, w-y_p, z_p)$. The sleeper width w here refers to the bottom width at the end of the sleeper. In the simulation process, the vertical movement of the sleeper simulation model is controlled in a servo mode to simulate the gravity of the sleeper.

4 TEST AND SIMULATION ANALYSIS

4.1 Test Analysis

Fig. 7 shows the curve of the lateral ballast resistance to dual-gauge sleepers. In China, setting the track deformation vector to 2 mm both ensures that the track does not produce excessive deformation accumulation and that temperature and pressure are not limited excessively. As such, most areas of China can be laid with this type of track.

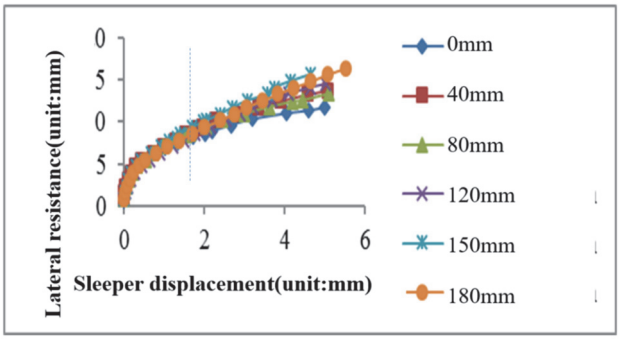

Figure 7 Displacement-resistance curve at different shoulder heights

According to China's railway standards, a sleeper displacement of 2 mm is the direct basis for determining the stability of a CWR. In this paper, the resistance in the event of a sleeper displacement of 2 mm is taken as the lateral ballast resistance, and the shoulder width is controlled at 500 mm, with the bed slope gradient at 1:1.75. With the step-by-step increase in shoulder height, the lateral resistance to dual-gauge sleepers increases by 0.63 kN, 0.04 kN, 0.07 kN, 0.12 kN and 0.38 kN, respectively.

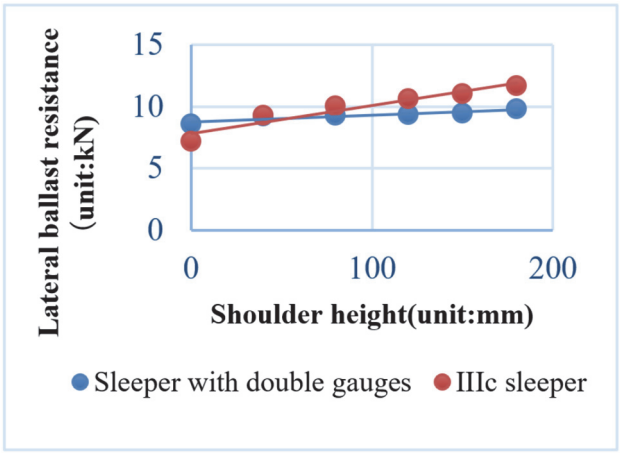

Figure 8 Comparison of resistance variation trends during step-by-step increase in shoulder height

Fig. 8 compares the variation trend of the lateral ballast resistance to dual-gauge sleepers and IIIc sleepers in the process of gradually increasing the shoulder height under the same test conditions. Compared with IIIc sleepers, the lateral resistance to dual-gauge sleepers is less influenced by shoulder height. The increase in lateral ballast resistance to dual-gauge sleepers, though less than that in IIIc sleepers, totals 2 kN/sleeper, which is important for maintaining the stability of the track. In addition, because increasing the shoulder height of the bed does not add much to the project cost, it is suggested that a shoulder height should be set at 180 mm for a dual-gauge railway track. A 60 kg/m rail should be used for the track railroad, which is 176 mm high, and the top surface is about 188 mm higher than the top surface of the sleeper (considering the 12 mm thick rubber pad under the rail). If the height is 190 mm, the ballast may

invade the limit and the safe operation of the train cannot be guaranteed. If it is less than 180 mm, the lateral resistance of the ballast bed will be reduced. Considering these factors, it is recommended that the shoulder height of the track bed be 180 mm.

Fig. 9 compares the variation trend of the lateral ballast resistance to dual-gauge railway sleepers and IIIc sleepers in the process of gradually decreasing the bed slope gradient under the same test conditions. It can be seen, that compared with IIIc sleepers, the lateral resistance to dual-gauge sleepers is less influenced by shoulder height. Where the slope gradient is the same, the lateral resistance to dual-gauge sleepers is 2~4 kN/sleeper, which is lower than the resistance to IIIc sleepers.

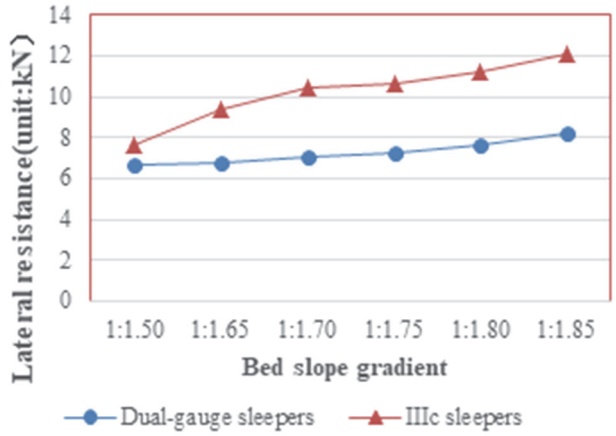

Figure 9 Comparison of resistance variation trends during a step-by-step decrease in slope gradient

Fig. 10 shows the schematic cross section of the embankment, where *B* is the width of the top surface of the roadbed, and *b* is the width of the road shoulder. Taking a single-track quasi-gauge railway in Africa as an example, the width *B* of the top surface of the subgrade in the straight section is 6.15 m, and the width of the road shoulder is 0.8 m. Generally speaking, the width of the top surface of the single-track railway subgrade of 1000 mm gauge is 5.1 m, and the width of the shoulder is 0.5 m. A shoulder width of 0.275 m can meet safe driving requirements. Therefore, if the meter-gauge railway is transformed into a 1435 mm/1000 mm set-gauge railway, the existing subgrade width can meet the driving safety requirements, and there is no need to widen it. When the shoulder width is insufficient due to special reasons, engineering measures such as adding a small shoulder retaining wall or laying concrete short piles can be used to solve the problem.

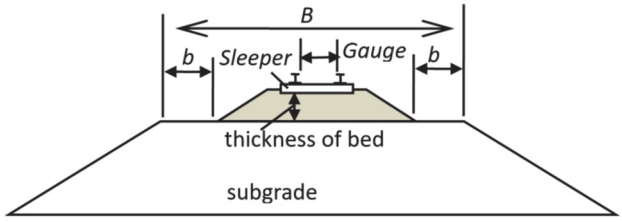

Figure 10 Cross section of embankment

Dual-gauge sleepers are generally used in sections where a metre-gauge railway is to be renovated into a standard-gauge railway. If the subgrade of the metre-gauge railway has a top width satisfactory for laying the dual-gauge railway track, there is no need to widen the subgrade. A steep bed slope is more suitable for a narrow subgrade top, which can be a prerequisite for not widening the subgrade. Therefore, it is suggested that the bed slope gradient should be set at 1:1.65 in dual-gauge track sections.

4.2 Simulation Analysis

In order to reveal the difference of lateral ballast resistance to dual-gauge sleepers and IIIc sleepers mesoscopically, the evolution law of force chains in bed during the process of lateral sleeper movement is studied to analyse the macro mechanical properties of lateral ballast resistance. With a shoulder width of 500 mm, a shoulder height of 150 mm, a bed slope gradient of 1:1.75, a sleeper burial depth of 150mm and a bed length of 600 mm[15], a simulation model of the dual-gauge sleeper-bed is built in PFC3D (see Fig. 11).

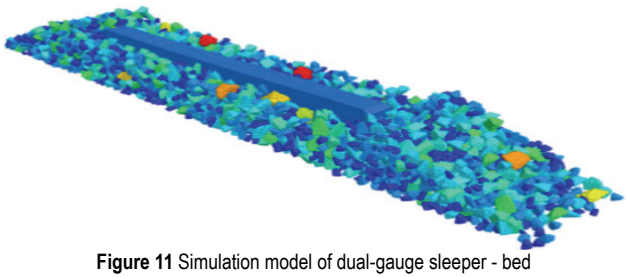

Figure 11 Simulation model of dual-gauge sleeper - bed

It is proposed to adopt CWR with a sleeper spacing of 600 mm in the track-covered railway, so the length of the track bed is taken as 600 mm. The particle clump, Clump, is used to simulate ballast. The wall element, Wall, is used to simulate a sleeper. In the figure, clumps are blue, green, yellow, orange and red, indicating that the ballast stress is increasing.

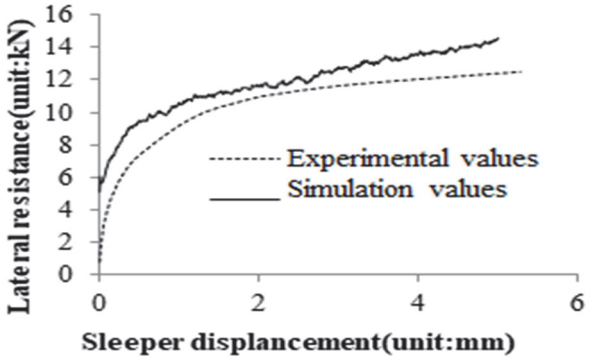

Figure 12 Comparison of simulation and test values of lateral resistance to dual-gauge sleepers

The simulation results of lateral ballast resistance to dual-gauge sleepers are shown in Fig. 12, and the simulation value is slightly greater than the test value. The reason for the difference is because the simulation employs the compactness after train rolling, while the bed can only be tamped in the test. The compactness of the bed not rolled by a train is relatively small, but in the bed simulation model, ballast particles sit tightly next to each other with little space in between. As a result, the compactness in the field and simulation tests varies. While the difference in bed compactness results in a difference between the test value and the simulation value, it is still generally

acceptable. In the figure, the curves of both the simulation and test results show that within a displacement of 1mm, the lateral resistance increases rapidly with displacement. There is a difference of 6.3% between the test value and simulation value in the event of a sleeper displacement of 2 mm. As such, the simulation result can be considered reliable, but the simulation value should be reduced by 6.3%.

The widely varying contact forces between ballast particles create a network of force chains of different thicknesses in the bed. A thick force chain has a large contact force, and a thin force chain has a small contact force. Fig. 13 shows the force chain distribution in the bed with a sleeper displacement of 5 mm. In the figure, force chains are blue, green, yellow, orange and red, indicating that the contact force of force chains is increasing. After a sleeper moves, the end away from the track centre has more thick force chains and a denser force chain network than the other end, which indicates that the shoulder has a significant impact on the lateral ballast resistance. In the figure, strong force chains incline downward, indicating that the force applied to the bed by a sleeper that moves laterally is not entirely horizontal. Evidence shows that the bed slope gradient has a significant impact on the lateral ballast resistance to sleepers.

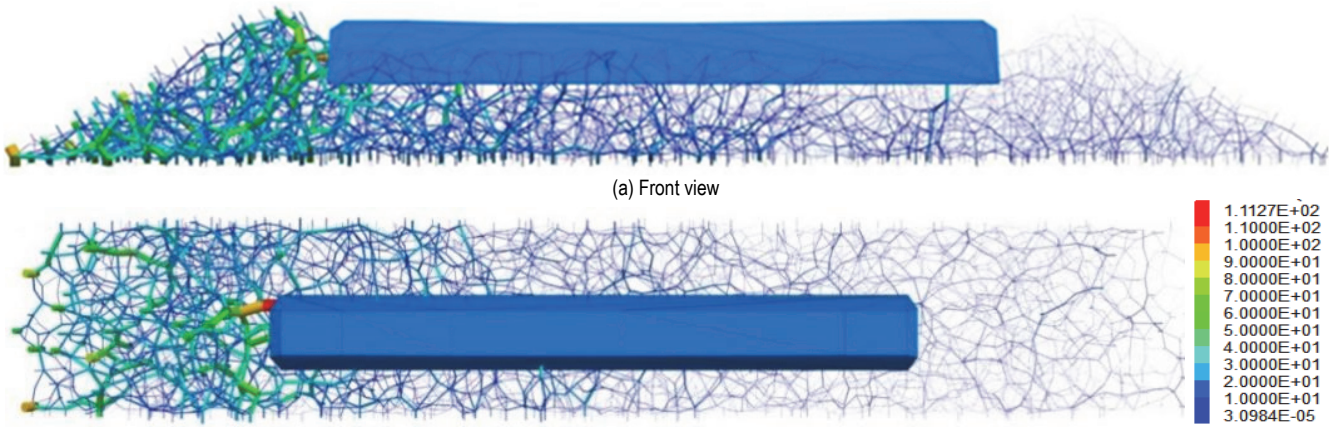

(a) Front view

(b) Top view

Figure 13 Force chain distribution in bed with dual-gauge sleeper displacement of 5 mm

According to the contact simulation, with a dual-gauge sleeper displacement of 2 mm, the lateral resistance (according to the revised value) shared by the bottom, ends and sides is 6.76 kN, 3.05 kN and 1.14 kN, accounting for 42.09%, 37.75% and 20.16%, respectively. In the same way, it is calculated that with a IIIc sleeper displacement of 2mm, the lateral resistance shared by the bottom, ends and sides is 5.94 kN, 5.32 kN and 1.14 kN, accounting for 47.93%, 42.91% and 9.16%, respectively.

Table 1 Lateral resistance sharing ratio of different contact surfaces of the two types of sleepers / %

	IIIc	Dual-gauge
Bottom sharing	47.93	42.09
End sharing	42.91	37.75
Side sharing	9.16	20.16

Tab. 1 lists the lateral resistance sharing ratio of different contact surfaces of the two types of sleepers. For dual-gauge sleepers, the side sharing ratio is more than twice that of IIIc sleepers, while the bottom and end sharing ratios are smaller in comparison to IIIc sleepers. This result is a smaller lateral ballast resistance to dual-gauge sleepers than to IIIc sleepers. The research results show that to increase the lateral ballast resistance to sleepers, the area of sleeper ends should be enlarged and the sleeper bottoms should be made rougher.

5 SLEEPER IMPROVEMENT

The original dual-gauge sleeper is optimised to form a jointed sleeper with side blocks in the middle (see Fig. 14).

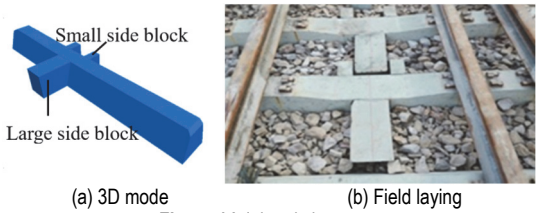

(a) 3D mode (b) Field laying

Figure 14 Jointed sleeper

In the test, side blocks are bonded to the sleeper sides with modified acrylate adhesive. The big side block is 200 mm long (in the sleeper's length direction), 291 mm wide (in the sleeper's width direction) and 225 mm high, which makes it level with the middle of the dual-gauge railway sleeper. The small side block is 90 mm long (in the sleeper's length direction), 90 mm wide (in the sleeper's width direction) and 225 mm high. The gaps between adjacent snap-in sleepers are filled with resin to relieve the impact between adjacent sleepers. In order to ensure the installation accuracy, the position deviation of the wing block along the length of the sleeper should be controlled within ±5 mm, and the reserved value of the gap between adjacent sleepers should be controlled within 20 mm ±5 mm. In order to verify the distribution of bed resistance to the jointed dual-gauge sleeper, a bed section with a slope gradient of 1:1.75, a shoulder width of 500 mm and a shoulder height of 150 mm is set at the test site. Then a resistance test is performed using the above test method.

Tab. 2 compares the lateral ballast resistance to the three types of sleepers. The lateral ballast resistance to jointed dual-gauge sleepers increases by 26.93% from that of the original dual-gauge sleepers, and the lateral ballast resistance to jointed sleepers is 8.4% greater than that of IIIc sleepers.

Table 2 Comparison of lateral ballast resistance to three types of sleepers / kN

Dual-gauge sleeper without side block	Jointed dual-gauge sleeper	IIIc sleeper
9.45	11.99	11.06

The test data show that the improvement idea is feasible and therefore provides a new solution for dual-gauge railway continuously welded rail sleepers.

6 CONCLUSIONS

It can be concluded from the simulation and test that:

(1) A ballast particle simulation model based on the discrete element method and using the convex hull algorithm can simulate the irregular shape of ballast particles without using a 3D scanner. Compared with test data, the simulation results from the ballast particle model built in this way are more accurate.

(2) The test results of side block-free dual-gauge sleepers show that the best solution to improve the lateral ballast resistance to dual-gauge sleepers is to enlarge the end area and further roughen the bottom.

(3) Under the premise of no increase in cost or a small increase in prefabrication cost, the lateral ballast resistance can be improved by optimising the sleeper size. By designing thick ends and a thin middle part, the lateral ballast resistance can be greatly improved, and the ballast can be limited in the crib. This is conducive to maintaining the lasting stability of the track. "Jointed" sleepers help greatly in increasing the lateral ballast resistance and improving the lateral rigidity of the track frame, thereby helping maintain the stability of the track.

7 REFERENCES

[1] Sadeghi, J. M., Zakeri, J. A., & Najar, M. (2016). Developing track ballast characteristic guideline in order to evaluate its performance. *International Journal of Railway*, *9*(2), 27-35. https://doi.org/10.7782/ijr.2016.9.2.027

[2] Esmaeili, M., Nuri, R., & Yousefian, K. (2017). Experimental comparison of the lateral resistance of tracks with steel slag ballast and limestone ballast materials. *Proceedings of the Institution of Mechanical Engineers, Part F: Journal Of Rail And Rapid Transit*, *231*(2), 175-184. https://doi.org/10.1177/0954409715623577

[3] Jing, G., Aela, P., & Fu, H. (2019). The contribution of ballast layer components to the lateral resistance of ladder sleeper track. *Construction and Building Materials*, *202*(MAR.30), 796-805. https://doi.org/10.1016/j.conbuildmat.2019.01.017

[4] Jing, G. Q., Aela, P., Fu, H. et al. (2020). Numerical and Experimental Analysis of Lateral Resistance of Biblock Sleeper on Ballasted Tracks. *International Journal of Geomechanics*, *20*(6). https://doi.org/10.1061/(ASCE)GM.1943-5622.0001689

[5] Kasraei, A., Zakeri, J. A., Esmaeili, M. et al. (2014). A numerical investigation on the lateral resistance of frictional sleepers in ballasted railway tracks. *Proceedings of the Institution of Mechanical Engineers Part F Journal of Rail and Rapid Transit*, *230*(2), 1-10. https://doi.org/10.1177/0954409714543507

[6] Jing, G., Aela, P., Fu, H. et al. (2020). Numerical and experimental analysis of lateral resistance of biblock sleeper on ballasted tracks. *International Journal of Geomechanics*, *20*(6), 116-128. https://doi.org/10.1061/(ASCE)GM.1943-5622.0001689

[7] Gao, L., Luo, Q., & Xu, Y. (2014). Effects of ballet bed section dimension on its lateral resistance. *Journal of Southwest Jiao tong University*, *49*(6), 954-960. https://doi.org/10.3969/j.issn.0258-2724.2014.06.004

[8] Wei, K., You, R., & Ma, H. (2020). Discrete element numerical simulation of lateral resistance of meter-gage railway ballast bed for concrete sleeper. *Journal of Railway Engineering Society*, *37*(5), 7-11. https://doi.org/10.3969/j.issn.1006-2106.2020.05.002

[9] Jing, G., Fu, H., Jia, W. et al. (2018). Macro-micro Analysis of Lateral Resistance for High Speed Railway Ballasted Track. *Journal of Railway Engineering Society*, *35*(9), 21-25. https://doi.org/10.3969/j.issn.1006-2106.2018.09.004

[10] Yang, X., Gao, L., Zhang, Y. R. et al. (2016). Discrete element method analysis of lateral resistance of fouled ballast bed. *Journal of Central South University*, *23*(9), 2373-2381. https://doi.org/10.1007/s11771-016-3296-5

[11] Wang, W., Song, S., Yan, H. et al. (2018). Experimental study on resistance characteristics of ballast bed in different stamping stages. *Journal of Central South University (Science and Technology)*, *49*(8), 2003-2008. https://doi.org/10.11817/j.issn. 1672-7207.2018.08.021

[12] Kasraei, A., Zakeri, J. A., Esmaeili, M. et al. (2014). A numerical investigation on the lateral resistance of frictional sleepers in ballasted railway tracks. *Proceedings of the Institution of Mechanical Engineers Part F Journal of Rail and Rapid Transit*, *230*(2), 440-449. https://doi.org/10.1177/0954409714543507

[13] Koike, Y., Nakamura, T., Haya, K. et al. (2014). Numerical method for evaluating the lateral resistance of sleepers in ballasted tracks. *Soils & Foundations*, *54*(3), 502-514. https://doi.org/10.1016/j.sandf.2014.04.014

[14] Xiao, J., Liu, G., Liu, J. et al. (2019). Parameters of a discrete element ballasted bed model based on a response surface method. *Journal of Zhejiang University - Science A: Applied Physics & Engineering*, *20*(9), 685-700. https://doi.org/10.1631/jzus.A1900133

[15] Ngamkhang, C., Feng, B., Tutumluer, E. et al. (2021). Evaluation of lateral stability of railway tracks due to ballast degradation. *Construction and Building Materials*, *278*(2), 122342. https://doi.org/10.1016/j.conbuildmat.2021.122

Contact information:

Shougang HUANG, PhD Student
1) Key Laboratory of Traffic Safety and Control of Hebei Province,
Shijiazhuang 050043, China
2) A.P. School of Traffic and Transportation,
Shijiazhuang Tiedao University, Shijiazhuang 050043, China
E-mail: huangshougang@sina.com

Jinjie CHEN, Professor
Hebei University of Water Resources and Electric Engineering,
Cangzhou 061001, China
E-mail: cjjwxq@126.com

Jianxi WANG, Professor
(Corresponding Author)
Key Laboratory of Roads and Railway Engineering Safety Control,
Ministry of Education, Shijiazhuang Tiedao University,
Shijiazhuang 050043, China
E-mail: qianxi-2008@163.com

Bin YAO, Senior Engineer
China Harbour Engineering Co., Ltd.,
Beijing 100027, China
E-mail: byao@chec.bj.cn

Yadong LI, Assistant Engineer
Shuohuang Railway Development Limited Liability Company,
Cangzhou 062350, China
E-mail: 1573521226@qq.com